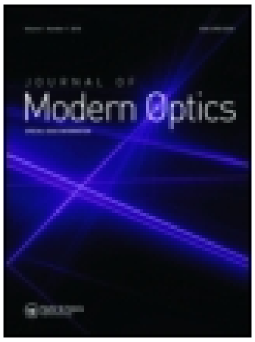

Journal of Modern Optics

ISSN: 0950-0340 (Print) 1362-3044 (Online) Journal homepage: http://www.tandfonline.com/loi/tmop20

Performance improvement of terrestrial free-space optical communications by mitigating the focal-spot wandering

A. ArockiaBazilRaj & Ucuk Darusalam

JOURNAL OF MODERN OPTICS, 2016
http://dx.doi.org/10.1080/09500340.2016.1200684

Performance improvement of terrestrial free-space optical communications by mitigating the focal-spot wandering

A. ArockiaBazilRaj[a] and Ucuk Darusalam[b]

[a]Electronics Engineering, Defence Institute of Advanced Technology, Pune, India; [b]Faculty of Information & Communications Technology, Informatics Engineering, Universitas Nasional, Jakarta, Indonesia

ABSTRACT

Focal-spot wandering is the main cause for the major power loss in free-space optical communications. Thus,mitigating it is a primary requirement for the successful performance improvement. In order to prove this prerequisite, an experimental set-up using 155-Mbps data transmission is built for the link range of 0.5 km at an altitude of 15.25 m. In the experiment, the receiver is equiped with a control system to stabilize the received optical propagation at the detector plane which is called as focal-spot wandering mitigation control so as to couple the power in bucket perfectly to the photodetector. The performance improvements due to mitigating focal-spot wandering are regressively investigated in terms of various quality assessment key parameters. Maximum radial distance of 0.25 mm, maximum effective scintillation index of 0.17, optical signal-to-noise ratio of 9 dB, minimum eye-opening of ±0.37 V, minimum eye-height of ±0.51 V, controlled bit-error-rate of 6.45×10^{-9} to 7.09×10^{-8} and the link margin of 1.83 dB are attained even during strong turbulence level while mitigating focal-spot wandering.

ARTICLE HISTORY
Received 28 May 2016
Accepted 7 June 2016

KEYWORDS
Free-space optical communications; focal-spot wandering; beam centroid displacement; effective scintillation index; OSNR; eyediagram; BER; link margin

1. Introduction

Free-space optical communications (FSOC) has become an essential part of modern information technology (*1–3*). This is due to various key features which include large, unregulated (free of government regulation) and licence-free transmission bandwidth spectrum, large data transmission (at the order of multiple gigabits per second), consumption of low power, security (cannot penetrate walls), low operational cost, quick deployment (smaller size and weight), last-mile access, fibre backup, back-haul for wireless cellular networks, high-definition television transmission as well as more freedom from electro-magnetic interference and electro-magnetic compatibility (*3–8*). Moreover, FSOC seems very appealing and a cost-effective solution (*1, 3, 8*) as it has the capability to meet the future network'sdemands (*9*) and provides ubiquitous and broadcasting services when compared to other networking technologies. FSOC is expected to have an important role in the future satellite networks, space and scientific explorations (*9–12*). The Portability of FSOC leads to establishing temporary links for high-speed information flows in big cities and industrial complexes (*2, 3, 9–11, 13*).

Despite these advantages, the successful deployment of FSOC has still remained a challenging task. Since, the transmission medium of FSOC is the atmospheric turbulent channel, its performance greatly depends on the local weather conditions (*4, 5, 9, 12*). This is primarily due to the unpredictable nature of FSOC channel effects at optical frequencies as well as difficulties associated with stabilizing the transmitting and receiving platforms against wind and other disturbing agents which affect the quality of received optical propagation (*4, 9, 14*). The optical propagation through the atmospheric turbulent channel severely suffers from atmospheric attenuation, angular deflection and phase distortion in horizontal (terrestrial) rather than vertical propagation (*9, 13, 15, 16*). Attenuation is described as photons being extinguished along propagation path. In the case of a laser beam, attenuation rather leads to a displacement of the excitation than to photons being extinguished. In addition to this, atmospheric turbulence also leads to phase-front distortions resulting in the deflection of incidentbeam (optical propagation) i.e. focal-spot wandering (FSW) (*7, 14, 16–18*). All of these effects result in both average received power loss and instantaneously received power fluctuation, called

CONTACT A. ArockiaBazilRaj brazilraj.a@diat.ac.in

fading, at the receiver aperture. This eventually leads to increase in the order of bit-error-rate(BER), decreased channel capacity and reliability of the overall system (5, 9, 19, 20). These effects interrupt the high data rate of FSOC link from achieving the availability of five nines 99.999% (9, 19, 21). One approach to address these problems is to increase the optical power level launched into the air when the propagation loss becomes high. However, the use of high-power optical amplifiers as boosters will increase the cost steeply (9). Another approach for reducing the optical power fading is to use slightly diverged beam and receive it via larger size aperture telescope (1, 6, 7, 9, 22). However, a diverged beam usually causes significant loss of average received power and increasing the aperture of the telescope will lead to collecting background radiations as well (1, 9, 11, 23). Therefore, the benefits of increasing the optical power and/or using slightly diverging beam with larger receiver aperture (larger than or close to the long-term laser spot size) may not balance FSOC performance loss/degradation (1, 8, 11, 15, 22).

Thus, immense research is being carried out in this domain, particularly with regard to the mitigation/compensation of signal degradation caused by turbulence effects. The major impact on FSOC data link due to the random fluctuations of the atmospheric turbulence is as follows: (i) optical scattering and observation (ii) random optical power fluctuation or scintillation (iii) FSW and (iv) wavefront distortions (5, 6, 9, 11, 12, 14, 15). The conventional data coding and/or modulation techniques can effectively be used to equalize/compromise the first two effects with respect to the weather condition at a given instant of time (9, 13). The third and fourth effects cannot be resolved without incorporating the elements of adaptive optics such as beam stabilization and correction of wavefront aberration (8, 10, 11, 16–19, 24). Resolving these problems is mandatory for the successful installation of FSOC (3, 9, 13, 14, 25). One of the major reasons for the failure of FSOC is the absence of beam pointing, acquisition and tracking system and thus, a perfect and continuous adaptive alignment is important to reduce the pointing loss (1, 9, 11, 14, 16, 23). To experimentally demonstrate this mandatory requirement for the successful installation of FSOC, a real-world open atmospheric optical data transmission system with necessary optoelectronic assembly comprising Transmitter (Tx) and Receiver (Rx), is required as portrayed in Figure 1. Using this set-up, a terrestrial experimental study is being carried out to characterize the performance of FSOC with and without mitigating FSW. The beam centroid radial distance (γ) (16), effective scintillation index (ESI) (24), eyediagram (19), BER and link margin (LM) are continuously measured and recorded. On and off line analysis are carried out as well in MATLAB environment in order to investigate

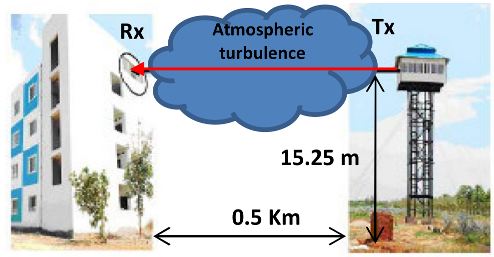

Figure 1. The receiver (Rx) and transmitter (Tx) in the range distance of 0.5 km at an altitude of 15.25 m.

intensively the performance improvement attained at the detector plane due to the deployment of focal-spot wandering mitigation (FSWM) control.

2. Terrestrial FSO data transmission experimental set-up

Simplex FSOC data link experimental set-up as shown in Figure 2, is built with necessary optoelectronics components for propagation path length of 0.5 km at an altitude of 15.25 m. The experimental test-bed consists of Pseudo Random Binary Sequence (PRBS) data source, NRZ data formatter, Continuous Wave (CW) laser source, Beta-Tx CW optical modulator, Pure Reflection Mirror (PRM), transmitting optics at the transmitter station and telescope, Fast Steering Mirror (FSM), Narrow-Band Interference Optical Filter (NBIOF), variable beam splitter, Optoelectronics Position Detector (OPD), error computation circuit, digital neuro-controller (9, 16, 25), D/A converter, piezo-amplifier, photodetector (PD), Trans Impedance Amplifier (TIA) and real-time oscilloscope at the receiver station. The FSM consists of three-terminal piezoelectric actuator-based moving platform on which a PRM is mounted (14, 24). All of the optoelectronics devices are mounted on the vibration-damped optical breadboards. A serial PRBS generator circuit of 213-1 is developed in the FPGA as described in (26), and its bit stream output is given as the input to the optical modulator. The optical signal from laser source at wavelength (λ) of 850 nm with power output of 10 mW CW is modulated by bit stream at the asynchronous transfer mode in the rate of 155 Mbps. Such a high data rate will not lead to using the beacon beam which is more commonly used to get the beam position and distortion information (6, 9, 11, 13, 24). However, using the beacon beam either as an adjacent beam or expanding along the propagation path steeply increases the cost of system (9).

NRZ-OOK scheme: bit stream of low (bit ‘0’) and high (bit ‘1’) unipolar NRZ signal, is used to directly modulate the optical signal (1, 4). The modulating signal amplitude has been set to 100 mVpp in order to achieve a fair

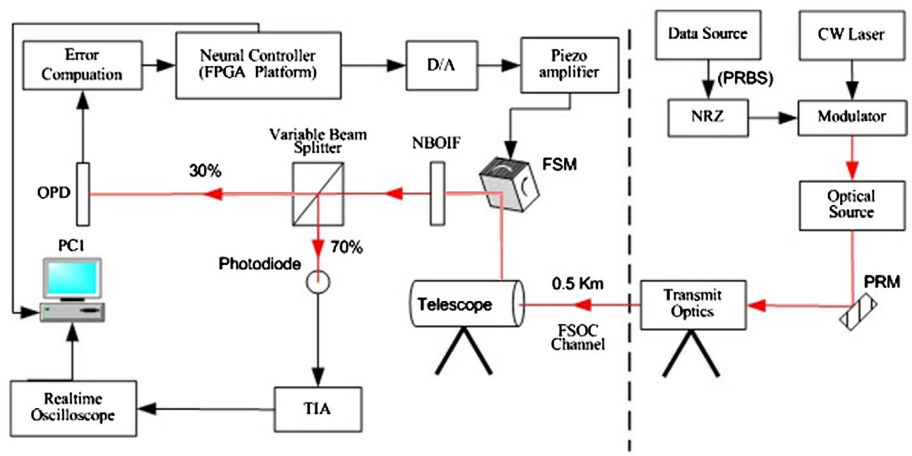

Figure 2. Schematic diagram for the experimental set-up of FSOC system.

comparison. The transmitting optics is used to increase beam diameter from 3 to 9 mm, in order to reduce beam divergence at the aperture of receiver (*1, 9, 19, 22*). The optical propagation from the transmitting optics is aligned such as to incident on the aperture of receiver through the real-world open atmosphere. The telescope captures all the optical power and reflects to fall on the FSM. The incident of optical propagationon is reflected to the beam splitter, through the NBIOF (*16*), which in turn splits the incident beam into reflection and forwarded optical propagation. The reflected beam is designed to fall on the PD followed by TIA and used for the assessment of communication key parameters. The equivalent photocurrent at the output of PD is amplified using a TIA. The output of the TIA is received by a high-frequency real-time oscilloscope through which the full signal analysis is carried out during different turbulence level: very weak to strong C_n^2 i.e. (10^{-16} to 10^{-12}) $m^{-2/3}$. The forwarded optical propagation (passed through the beam splitter) is received by the OPD where signal conditioning and error computation circuit are implemented to measure the error. Henceforth, the error data are given to neural-controller developed in the FPGA (*24*). The controller output data are converted to analogue signal using D/A converter and given to the FSM through the piezo-amplifier in a closed-loop control configuration as described in (*16, 23*). The telescope eye-piece output beam (collimated) with diameter of 4mm is initially centred at the optimal point of the OPD i.e. (0, 0) mm (*16, 24*). Therefore, the maximum centroid displacement distance on both sides of the 2D plane of OPD is ±2mm. The OPD could not yield the position information once the beam centroid is off by 2mm on both sides and under this condition, the neuro-controller loses its controllability (*14, 16, 23, 24*). However, the beam is stabilized immediately once the beam centroid slightly moves off the centre of OPD by steering the beam back to optimal point using the neuro-controller in closed-loop control and it no longer lets the beam move or being locked precisely. The measurement data, beam pointing stability and quality metrics of data link are continuously monitored and analysed using personal computer (PC1). Descriptions on the beam position measurement, error computation method and design/implementation of neuro-controller can be found in our recent publications (*16, 24*) and (*25*), respectively.

3. Experimental results

Performance improvement attained on the quality and reliability of FSOC data link by mitigating FSW is evaluated in terms of γ, ESI, optical signal-to-noise ratio (OSNR), eyediagram, BER and LM during different outdoor environmental conditions. Some of the experimental data obtained at the test field with and without mitigating FSW are analysed through which the impact of the beam wandering in terrestrial FSOC is analysed in this section.

3.1. Analysis of beam centroid stabilization and ESI

The radial distance (γ) of the received optical propagation is continuously measured, as detailed in (*16*), using the beam centroid displacement on the OPD-2D plane. The surface plots of the measurement results corresponding to 50,000 data samples obtained in different weather conditions (winter, summer and rainy) are shown in Figure 3(a)–(d). The first plot is designed with the data measured when FSWM control is in off condition while the other plots are designed when the control is in on. The important observations in no-control from Figure 3(a) are (i) variations of the γ are highly arbitrary, since, each point of the surface plot is measured several times with the random count values, (ii) beam centroid wanders almost exist at all the areas of the OPD plane and (iii) sometimes

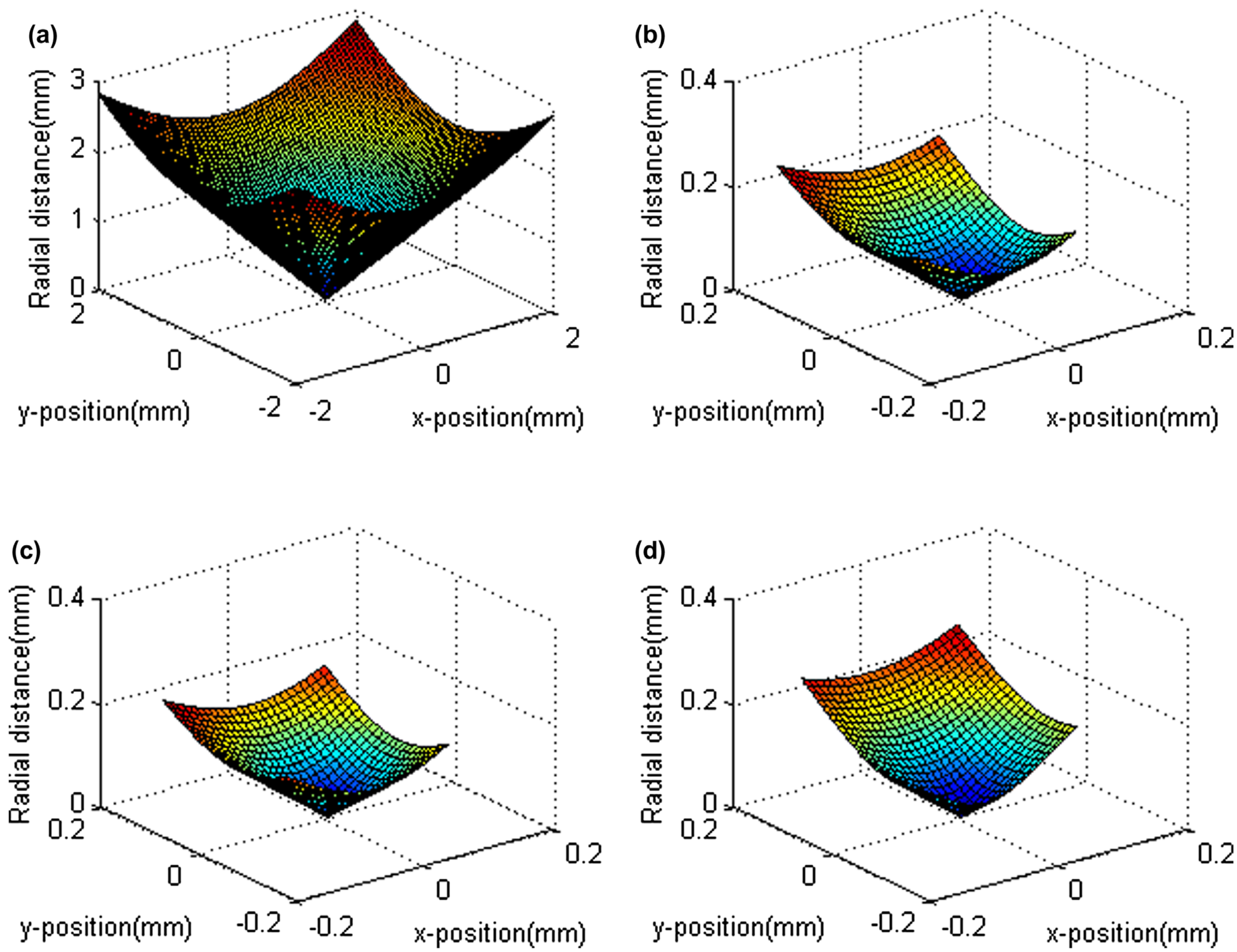

Figure 3. Surface plots of radial distance on the OPD against measured x and y position errors.

the beam centroid goes out from the detector plane and, under this condition, FSOC link is broken. Further, the perfect coupling of power in bucket (PiB) to PD becomes difficult and unreliable, it leads to wide range of power fluctuation at the PD and thus it yields severe degradation in the overall performance of FSOC.

The interesting observations in FSWM control from Figure 3(b)–(d) are as follows: (i) beam centroid movement is effectively controlled and the values of the γ are always around the optimal point, (ii) very narrow range of power fluctuations are seen at the PD and (iii) maximum intensity of received optical propagation (the Gaussian beam) i.e. PiB is perfectly coupled to the PD and an unbroken FSOC data link is achieved. The min–max values of position errors (Ex, Ey) (*16, 24*) and their corresponding γ are −0.15 to 0.1 mm, −0.1 to 0.18 mm and 0.1 to 0.24 mm; −0.14 to 0.11 mm, −0.1 to 0.15 mm and 0.1 to 0.20 mm and −0.1 to 0.14 mm, −0.05 to 0.19 mm and 0.05 to 0.23 mm for winter (trial1), summer (trial 2) and rainy (trial 3), respectively. A similar pattern is observed in the other seasons as well. These results clearly show evidence of the significance of mitigating FSW to perfectly couple the instantaneous amplitude, i.e. the point of maximum intensity to the PD.

The power fluctuation of the received optical propagation is continuously measured using the PD output signal (V_{Rec}) with FSWM control off and on conditions through which the corresponding ESI is computed. The ensemble average (*17, 22, 25*) of V_{Rec} used to estimate the ESI as $\left\{\left(\langle V_{Rec}^2\rangle/\langle V_{Rec}\rangle^2\right)-1\right\}$ (*9, 25*) and a portion of the estimated time series results for three weather conditions are shown in Figure 4(a). Therein, FSWM control is kept off until 10.30a.m. and then turned on. It is clearly seen from Figure 4(a) that, the ESI fluctuations exhibit the broader (outer scale) variations from 0.53 to 1.86 i.e. 28.49 to 96.84% when FSWM control is off, whereas in on condition, ESI fluctuations fell within the inner-scale with the min–max values of 0.03 and 0.15 i.e. 1.61 to 6.45%. These results exhibit the improvements which are attained in the stability of the received signal by mitigating FSW.

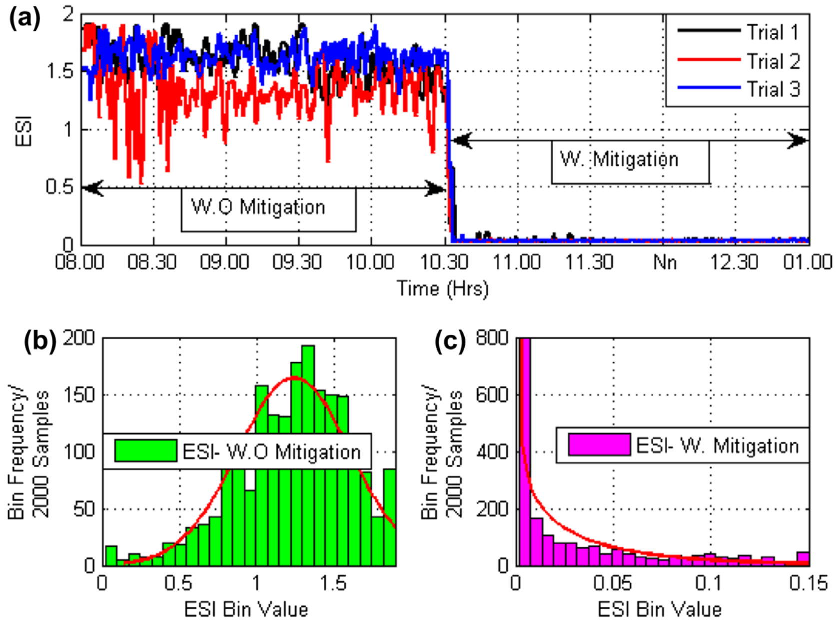

Figure 4. The estimation of ESI using ensemble average of PD output signal.

The ESI fluctuations, even with beam steering control, do not reach exactly zero and they reach a maximum of 0.15. This is purely due to the scintillation effect on the optical propagation (*9, 20*), as explained in section 1, which could not be controlled by the steering system but can be resolved using the conventional data coding technique and/or adaptive gain control circuit (*3–5, 8, 9, 21*) which form/is the matter of subsequent research.

The histogram plots as shown in Figure 4(b) and (c) are generated with 2000 ESI sample data obtained from the experiment conducted with FSWM control in its off and on conditions, respectively. The main observations from Figure 4(b) are that (i) ESI values occupied all bins, (ii) maximum counts are obtained for the bin values of 1 to 1.65, (iii) minimum counts are obtained for bin values of 0.1 to 0.7 and (iv) data distribution reasonably fits with the Gaussian function with different mean values.

The interesting observations from Figure 4(c) are that (i) ESI values occupied the lowest bin values i.e. 0.03 to 0.15, (ii) maximum counts are obtained for optimal bin and values around it, (iii) minimum counts are obtained starting from 0.05 onwards and it reaches zero count value after 0.15 and (iv) data distribution closely fits with the Gamma function. These results clearly show evidence that the beam centroid is almost around optimal point when FSW is well controlled. Almost, similar results have been obtained from the experiment conducted for longer periods during different weather conditions. Therefore, mitigating FSW improves reliability of FSOC link. The OSNR is estimated as 10 log 10(s/n) in dB using linear optical signal (s) and noise (n) powers that are measured at receiver while FSWM control is in off and on conditions.

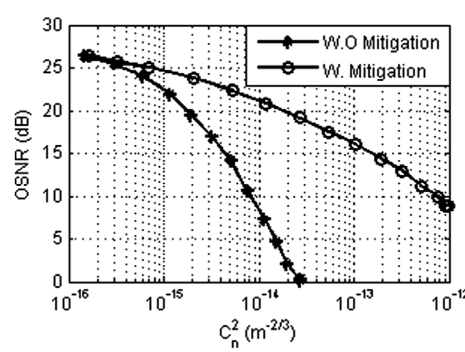

Figure 5. OSNR against different atmospheric conditions.

The experimental results obtained during different level of C_n^2 (*20*) are shown in Figure 5 and therein, the OSNR researches 0 dB drastically as the C_n^2 increases when FSW is not mitigated, whereas in the other case, the OSNR decrement pattern is abruptly changed with the greatest slope difference and an improved response is observed. For example, the OSNR achieves 0 dB for the C_n^2 value of $1.9\times 10^{-14}\mathrm{m}^{-2/3}$ when FSW is not mitigated and on the contrary, by mitigation, the OSNR value for the same C_n^2 value is 19.3 dB. Furthermore, the value of OSNR even during strong turbulence level $C_n^2 = 10^{-12}\mathrm{m}^{-2/3}$ is 8.34 dB while FSWM is turned on. Therefore, once FSW is not mitigated, the OSNR becomes lower due to more beam centroid outages on PD, thus deciding the correct bit at the receiver station becomes difficult. Further, these results show that FSW increases irradiance fluctuations and causes an effective pointing error that leads to larger values of scintillation index as predicted by Rytov theory (*9, 17*).

The amount of reduction in scintillation index when the incident of optical propagation is tracked depends on the accuracy of tracking method/system (6, 9, 24). If the incident of optical propagation is tracked, the on-axis scintillation index more closely matches Rytov theory, otherwise it is beyond estimation (17, 22). Therefore, FSW has to be mitigated in order to reduce the irradiance fluctuations so as to maintain the value of scintillation index more close to Rytov prediction (9).

3.2. Influence of beam wandering on optical communication signal

In order to quantify the impact of FSW on OOK-NRZ modulatedoptical signal (9) at the test field during different turbulence level (C_n^2) the eyediagram is constructed with FSWM control in on and off conditions, as depicted in Figure 6. The eyediagrams are constructed using a MATLAB comment 'eyediagram (x, *n*)'; where, x representsthe samples of received signal and n is the number of samples plotted in each trace. In Figure 6, the first row corresponds to FSWM control in off condition, while the second row to on condition.

The main observations from the first row are (i) FSWM control is not required during very weak turbulence level, $C_n^2 = 10^{-14}$ since FSW effect is almost zero, (ii) eye height as well as eye-opening has started decreasing from weak level onwards, (iii) FSW integrated effect increases as the C_n^2 increases, (iv) eye-opening becomes 0V during strong turbulence level $C_n^2 = 10^{-12}$ condition, (v) the noise becomes the dominant factor and the output signal level gets saturated in the upper regime of C_n^2 and (vi) normalized values of eye-opening during different C_n^2 are ±0.92, ±0.73, ±0.32 and ±0, whereas in the other case, (i) eye-amplitude as well as eye-opening is significantly improved, (ii) maximum improvement is attained during weak and strong turbulence level, (iii) the received signal power fluctuation is in a way analogous to the Rytov variations i.e. scintillation index and (iv) the normalized values of eye-opening during different C_n^2 are ±0.92, ±0.81, ±0.58 and ±0.37. These results clearly show evidence that FSW has to be mitigated to improve the Q-factor, OSNR, reduce the order of BER and correctly decide the received bit. The distribution patterns (histograms) are designed using 2000 ensembles corresponding to the signal obtained from the output of the TIA when FSWM control is in 'off' and 'on' conditions where the decision threshold (I_{th}) level is selected to be 0V, as shown in Figure 7(a) and (b) respectively.

The received signal distribution for bits '1' and '0' are equally spaced and comparable for both sides of I_{th} level

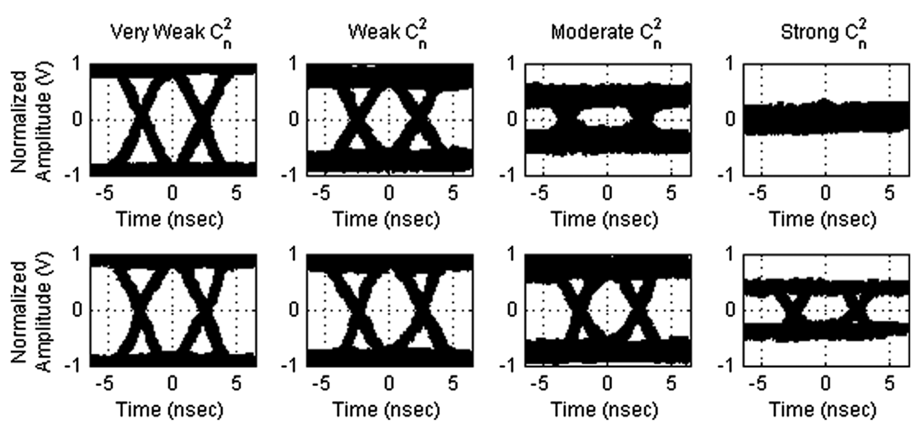

Figure 6. Eye diagram obtained during different turbulence level C_n^2 values for very weak to strong turbulence level. Note that the *y*-axis is normalized to the maximum output voltage.

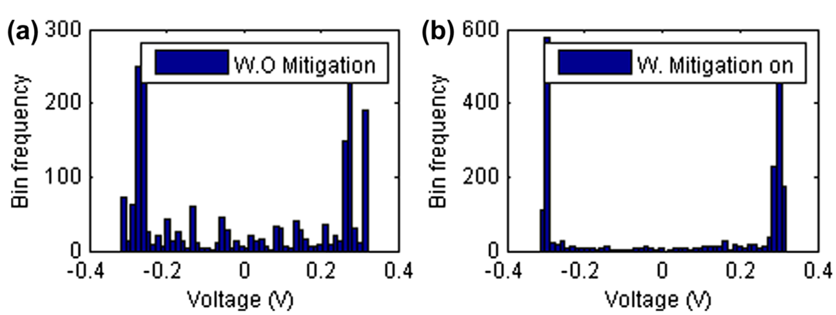

Figure 7. Histogram of OOK-NRZ received signal.

and the bits '1'and '0' are clearly distinguishable in the presence of FSWM control even during strong turbulence level as in Figure 7(b), whereas in the absence, the received signal distribution becomes heavily distorted as in Figure 7(a) and is no longer distinguishable during strong turbulence level $C_n^2 = 10^{-12}$ conditions which result in the decreased Q-factor, OSNR and increased BER values. As in Figure 7(a), the maximum count value of ≈290 for bit '0' at −0.28V and the same count value for bit '1'at 0.25V with many voltage level distributions in between these two levels are observed when FSWM control is off, whereas in on, the maximum count value of ≈590 for bit '0' at −0.3V and ≈490 for bit '1' at 0.3V with the ≈0V distribution in between these two levels are observed even during the strong turbulence level, $C_n^2 = 10^{-12}\text{m}^{-2/3}$.

3.3. Numerical analysis of FSOC reliability

The BER performance improvement is investigated using the Keysight N4902B serial BER tester in a daylong operation by alternatively switching FSWM control on and off in time span of 60seconds and simultaneously BER values are recorded. A portion of the experimental results obtained over 600 runs in total measurement time span of 10 minutes is shown in Figure 8. Note that the zero BER is truncated to smallest possible non-zero value of 6.45×10^{-9}. As shown in Figure 8, BER measured without FSWM control reaches the maximum of four orders of magnitude higher than the measurements obtained with FSWM control. The BER varies in the inner-scale and it is controlled within 6.45×10^{-9} (1 error bit) and $\approx 7.09 \times 10^{-8}$ (11 error bits) with the mean value of 3.86×10^{-8} which is less than 10^{-6} in the presence of FSWM control, whereas in its absence, the BER varies in the outer-scale and measured min–max values are 7.89×10^{-7} (122 error bits) and 1.6×10^{-2} (2,500,000 error bits) with the mean value of 8×10^{-3}.

These results exhibit quality and reliability improvements attained in terrestrial FSOC data link. Based on those, results also show clear evidence that sustaining FSOC data link with the lowest BER during different C_n^2 conditions is possible only with mitigating FSW effects. The LM is estimated by using the average transmitted optical power (Pt) of 10 mW, PD sensitivity (Spd) of 0.59 A/W@155Mbps, fluctuating atmospheric turbulence loss (Ltur) (*22*), constant geometrical loss (Lgeo) of 0.0023 mW and pointing error (Lpe) as Pt + Spd-Ltur-Lgeo-Lpe (*3, 4, 9*). The estimation of LM is carried out in the presence and absence of FSWM control and the results are shown in Figure 9. In the presence of FSWM control, the fourth term i.e. Lpe of LM estimation becomes negligible i.e. almost zero during the experimentation and hence, the LM becomes a function of only one variable i.e. Ltur which is measured using the received signal (*22*). As it is observed in Figure 9, the LM steeply goes down with respect to the received power loss during different C_n^2 values. The decreasing pattern is abrupt once FSW is not mitigated, whereas in the other case, the pattern is significantly improved. For example, the value of LM is 3.8 dB in the absence of FSWM control when the $C_n^2 = 10^{-14}\text{m}^{-2/3}$ and in its presence the value is 6.02 dB. Further, the value of LM is 0 and 1.83 dB when FSWM control is in off and on conditions respectively,while the condition is strong turbulence level, $C_n^2 = 10^{-12}\text{m}^{-2/3}$.

The experimental results obtained during different local seasons suggest that a reliable FSOC data link can be established for propagation path length of 7 km with FSWM control at data rate of 155 Mbps during different C_n^2 conditions i.e. very weak through strong regimes using the optoelectronics assembly as shown in Figure 2. However, the performance of FSOC data link deteriorates drastically (BER increases to $\approx 10^{-2}$) as the C_n^2 increases to the upper regime of strong i.e. very strong ($C_n^2 > 10^{-12}\text{m}^{-2/3}$) conditions. Occasionally, maintaining the link availability was difficult and connectivity dropped down during the very strong turbulence level due to the wavefront aberration.

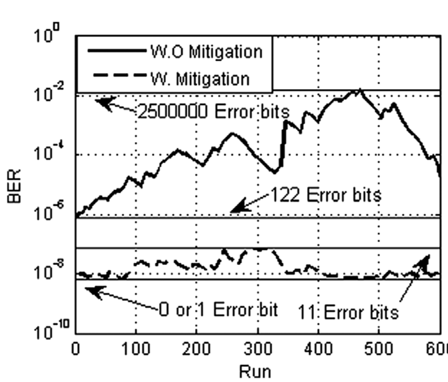

Figure 8. The measurement of BER through running time span of 60seconds over 600 runs.

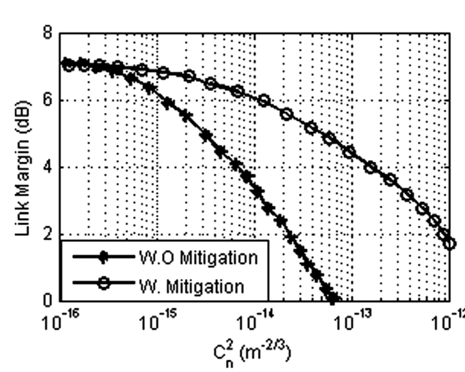

Figure 9. LM values against the different C_n^2 values.

Therefore, incorporating the high-speed signal conditioning circuit and adaptive optics: wavefront tip-tilt correction (*9, 10*) becomes necessary to improve the reliability of FSOC data transmission system further even during very strong turbulence level, which is set for the near future research work.

4. Conclusion

The turbulence effects of atmospheric channel influences the optical propagation on FSOC and the urgency for implementing FSWMhas been explained. The construction of FSOC experimental set-up which implements FSWM control has been described as well. Maximum γ of 0.25 mm, maximum ESI of 0.17, minimum OSNR of 9 dB, minimum eye-opening of ±0.37 V and minimum eye-height of ±0.51V are attained by mitigating FSW. The lowest BER value (one bit error) is obtained even for $1 \times 10^{-14}\mathrm{m}^{-2/3} \leq C_n^2 \geq 6 \times 10^{-14}\,\mathrm{m}^{-2/3}$ the presence of FSWM control. BER is significantly controlled for the min–max variations are 6.45×10^{-9} and 7.09×10^{-8}, respectively. These are observed in the day-long performance measurement. Further, the LM is estimated as a function of Ltur (nullifying the pointing error loss) and found that this FSOC system is capable of accomplishing data communication for the maximum propagation path length of 7 km. Therefore, the carried out experiment that has been demonstrated shows performance improvement, that the mitigation of FSW in FSOC using FSWM control significantly increases coupling efficiency of PiB into the PD so as to improve the overall quality and reliability of data transmission system during different outdoor environmental conditions.

Disclosure statement

No potential conflict of interest was reported by the authors.

References

(1) Raj, A.A.; Padmavathi, S. Statistical Analysis of Accurate Prediction of Local Atmospheric Optical Attenuation with a New Model According to Weather Together with Beam Wandering Compensation System: A Season Wise Experimental Investigation. *J. Modern Opt.* **2016**, *63* (13), 1–16, http://dx.doi.org/10.1080/09500340.2016.1140840

(2) Arimoto, Y. Developing a New Free-space Optical Communication Terminal that Realizes High-speed Broadband Communications. *NICT News* **2010**, *392*, 1–5.

(3) Khalighi, M.A.; Uysal, M. Survey on Free Space Optical Communication: A Communication Theory perspective. *IEEE Communication surveys and tutorials.* **2014**, *16* (4), 2231–2258.

(4) Arockia Bazil Raj, A.; Padmavathi, S. Quality Metrics and Reliability Analysis of Laser Communication System. *Defence Sci. J.* **2016**, *66* (2), 175–185.

(5) Mahdieh, M.H.; Pournoury, M. Atmospheric Turbulence and Numerical Evaluation of Bit Error Rate (BER) in Free-space Communication. *Opt. Laser Technol.* **2010**, *42* (1), 55–60.

(6) Andrews, L.C.; Phillips, R.L. *Laser Beam Propagation Through Random Media*. SPIE Press: Washington, **2005**.

(7) Anthonisamy, A.B.R.; Padmavathi, D.; Paul, L.J. Performance Analysis of Free Space Optical Communication in Open Atmospheric Turbulence Conditions with Beam Wandering Compensation Control. *IET Commun.* 2016, 1–16. http://dx.doi.org/10.1049/iet-com.2015.0717. http://ietdl.org/t/QfY$4b.

(8) Matsumoto, M.; Kazaura, K.; Dat, P.; Shah, A.; Omae, K.; Suzuki, T.; Wakamori, K.; Higashino, T.; Tsukamoto, K.; Komaki, S. *An Alternative Access Technology for Next Generation Networks Based on Full-optical Wireless Communication Links*. Innovations in NGN: Future Network and Services, 2008. K-INGN, First ITU-T Kaleidoscope Academic Conference, Geneva, 2008, 221–228.

(9) Arockia Bazil Raj, A. *Free Space Optical Communication: System Design, Modeling, Characterization and Dealing with Turbulence*. De Grutyer: Germany, 2016, http://www.degruyter.com/view/product/465377

(10) Li, M.; Cvijetic, M. Coherent Free Space Optics Communications Over The Maritime Atmosphere With Use of Adaptive Optics for Beam Wavefront Correction. *Appl. Opt.* **2015**, *54* (6), 1453–1462.

(11) Mohan, S.; Alvarez-Salazar, O.; Birnbaum, K.; Biswas, A.; Farr, W.; Hemmati, H.; Johnson, S.; Ortiz, G.; Quirk, K.; Rahman, Z.; Regher, M.; Rizvi, F.; Shields, J.; Srinivasan, M. Pointing, Acquisition, and Tracking Architecture Tools For Deep-space optical Communications. *Proc. SPIE* **2014**, *8971*, 1–11.

(12) Arockia Bazil Raj, A.; Lancelot, J.P. Seasonal Investigation on Prediction Accuracy of Atmospheric Turbulence Strength with a New Model at Punalkulam, Tamil Nadu. *J. Opt. Technol.* **2016**, *83* (1), 73–89.

(13) Arockia Bazil Raj, A., Mono-pulse tracking system for active free space optical communication. *Optik – Int. J. Light Elect. Opt.* **2016**, 1–12. http://www.sciencedirect.com/science/article/pii/S0030402616305964

(14) Raj, A.A.B.; Selvi, J.A.V. Lower-order Adaptive Beam Steering System in Terrestrial Free Space Point-to-point Laser Communication Using Fine Tracking Sensor. *IEEE Int. Conf. Signal Proc. Commun. Comput. Networking Technol.* **2011**, 699–704.

(15) Feng, F.; White, I.H.; Wilkinson, T.D. Aberration Correction for Free Space Optical Communications Using Rectangular Zernike Modal Wavefront Sensing. *J. Lightwave Technol.* **2014**, *32* (6), 1239–1245.

(16) Raj, A.A.B.; Selvi, J.A.V.; Kumar, D.; Sivakumaran, N. Mitigation of Beam Fluctuation Due to Atmospheric Turbulence and Prediction of Control Quality Using Intelligent Decision-making Tools. *Appl. Opt.* **2014**, *53* (15), 3796–3806.

(17) Raj, A.A.B.; Selvi, J.A.V.; Raghavan, S. Real-time Measurement of Meteorological Parameters for Estimating Low-altitude Atmospheric Turbulence Strength C_n^2. *IET Sci. Meas. Technol.* **2014**, *8* (6), 459–469.

(18) Ucuk, D.; Purnomo Sidi, P.; Eko Tjipto, R. Optical Spatial Filter to Suppress Beam Wander and Spatial

Noise Induced by Atmospheric Turbulence in Free-space Optical Communications. *Adv. Opt. Technol.* April **2015**.
(19) Wolfgang, F.; Rene, S.; Bernd, N.; Marcus, W.; Arne, J.; David, H.; Swen, K.; Joachim, M.; Michael, D.; Micheal, H.; Christina, K.; Juergen, B.; Juerg, L. *Quality Metrics for Optical Signals. Eye Diagram, Q-factor, OSNR, EVM and BER*. 14th International Conference on Transparent Optical Networks, Coventry, **2012**, 1–4.
(20) Raj, A.A.B.; Selvi, J.A.V.; Durairaj, S. Comparison of Different Models for Ground-level Atmospheric Turbulence Strength (Cn^2) Prediction With a New Model According to Local Weather Data for FSO Applications. *Appl. Opt.* **2015**, *54* (4), 802–815.
(21) Kevin, S.; Dirk, G.; Ramon, M.-C.; Florian, M.; Christian, F.; Christopher, S.; Joachim, H.; Jack, Y.; Vevek, S.; Ranjoy, B. *Channel Characterization for Air-to-ground Free-space Optical Communication Links*. Proc. of SPIE, San Francisco, CA, USA, vol. 8971, 1-13, 2014.
(22) Raj, A.A.B.; Selvi, J.A.V. Comparison of Different Models for Ground-level Atmospheric Attenuation Prediction with New Models According to Local Weather Data for FSO Applications. *J. Opt. Commun.* **2015**, 36 (2), 181–196.
(23) Raj, A.A.B.; Selvi, J.A.V.; Sathiya, R.; Shanthi, A.; Sharmila, M. Low Cost Beam Steering System for FSOC to SMF Coupling. *IEEE Int. Conf. Adv. Eng. Sci. Manage.* **2012**, 49–54.
(24) Raj, A.A.B.; Selvi, J.A.V.; Kumar, D.; Raghavan, S. Design of Cognitive Decision Making Controller for Autonomous Online Adaptive Beam Steering in Free Space Optical Communication System. *Wireless Personal Commun.* **2015**, *84* (1), 765–799.
(25) Raj, A.A.B.; Selvi, J.A.V.; Durai, K.D.; Singaravelu, R.S. Intensity Feedback-based Beam Wandering Mitigation in Free-space Optical Communication Using Neural Control Technique. *EURASIP J. Wireless Commun. Networking*. **2014**, 1–18. doi: http://dx.doi.org/10.1186/1687-1499-2014-160
(26) Muthiah, D.; Arockia Bazil Raj, A. Implementation of High-speed LFSR Design With Parallel Architectures. *IEEE Int. Conf. Comput. Commun. Appl.* 2012, 1–6.